Comparative Analysis of Davis Tube and Wet Low Intensity Magnetic Separation (WLIMS) Performance of Two Magnetite Ores

N. Maistry[1]; A. Singh[2]

1. Senior Engineer MSc. (Eng.)(Met.), Mintek, South Africa. Email: nicholem@mintek.co.za

2. Senior Technical Specialist: Physical Separation (PhD. (Eng.)(Chem.); Pr. Eng), Mintek, South Africa. Email: ashmas@mintek.co.za

1. INTRODUCTION

Magnetite is a ferromagnetic iron ore, typically found in igneous and metamorphic deposits, primarily used in steel making and coal washing. The demand for magnetite is dictated by the steel industry; however, growth is spurred by magnetite's high iron content as the industry shifts towards more energy efficient and lower emission production.

Pre-concentration of magnetite is achieved through magnetic separation, specifically low intensity magnetic separation (LIMS) as magnetite is ferromagnetic. When size fractions below 1mm are treated, Wet LIMS (WLIMS) is used to improve separation and minimize dust losses. The most common WLIMS used for cleaning of DMS medium and concentrating fine iron ore are drum separators. Separation is achieved by passing particles, which may or may not be in suspension, through a magnetic field. Magnetic particles are picked up by the magnet, resulting in magnetic material being retained on the magnet, until they exit the magnetic field, with only non-magnetics reporting to the tailings. Water is also used to ensure the pulp is in suspension (Svoboda, 2010). This operating principle is presented in Figure 1.

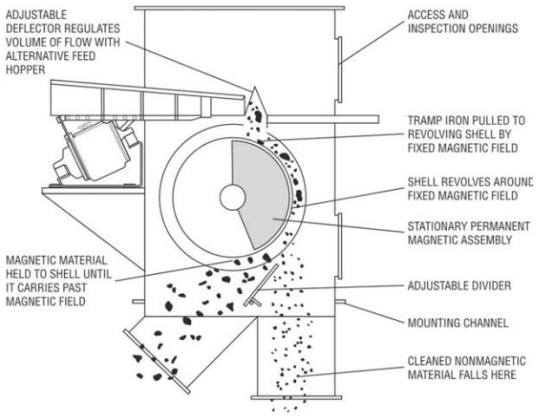

Figure 1: Operating principle of drum separator (Eriez, 2024)

Prior to WLIMS testwork, Davis tube testwork is performed to determine the degree of magnetic susceptibility of a material. The Davis Tube (DT) is a laboratory-scale equipment that assesses the amenability of an ore to magnetic separation via LIMS. It is only capable of handling small samples and it separates them into either ferromagnetic/strongly magnetic fractions or paramagnetic/weakly magnetic and non-magnetic fractions (Murariu & Svoboda, 2003). The Davis tube was developed in 1921 and there have been no significant design changes since then (Svoboda, 2010). It consists of a cylindrical glass tube that is supported at an incline, in between the two poles of a powerful electromagnet. Figure 2 indicates that during testing, the tube is filled with normal water and a prepared sample is added. The tube then oscillates to reject weakly magnetic and non-magnetic particles until complete separation is achieved (Schulz, 1963). In terms of operation, Schulz (1963) indicated that the magnetic induction between the poles should be at least 0.4 T. Whereas Steiner & Böhm (2000) suggested that DT testwork should be performed at a magnetic induction equivalent to the magnetic induction of the separator. However, this is incorrect as the magnetic force, not the field gradient, is responsible for separation. Finally, Murariu & Svoboda (2003) conducted extensive modelling of magnetic force patterns created by the DT and drum separators. They concluded that the magnetic induction of 0.1 T is required for traditional ferrite drum magnetic separators, with a 25 mm gap between the drum and the tank. (Svoboda, 2010).

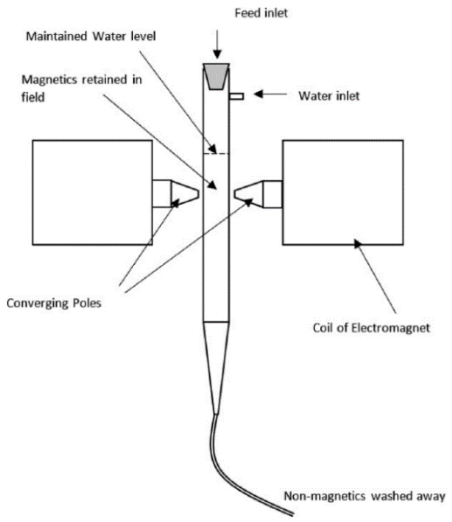

Figure 2: Davis tube operating principle (Jain, et al., 2016)

However, as with the scale-up of any operation, there are usually inefficiencies observed when transitioning from DT to WLIMS. Schulz (1963) concluded that a minimum magnetic field intensity of 4000 Gauss is required during DT testwork when benchmarking against drum separators. In comparison, Steinhart and Boehm (2000) indicated that the DT magnetic field intensity should be equivalent to that on the surface of the drum, which is usually 1000 Gauss. However, Murariu and Svoboda (2003) states that both arguments are incorrect as separation efficiency cannot be determined by the magnetic field strength alone. The efficiency of separation is determined by the product of the magnetic induction (B) and the field gradient (∇B), and this relationship is referred to as the force index ($FI = B\nabla B$). This indicates that the magnetic field gradients of DT and drum separators are different, thus, their resulting force index will be different. Furthermore, to ensure efficient separation of magnetics in a drum separator, the required force index must be generated at a sufficient distance from the surface of the drum. It is standard practice to specify the field strength at a distance of 50mm from the surface of the drum, however, the gap is approximately 25mm in industrial applications. This operating gap is dependent on drum diameter, ranging from 14mm for a 610mm drum diameter, to 40mm for a 1200mm drum diameter. In addition, the force index has an inverse relationship with distance from the surface of the drum, thus, DT testwork performed according to Steinert and Boehm (2000) cannot be directly applied to WLIMS (Murariu & Svoboda, 2003).

Murariu and Svoboda (2003) performed theoretical modelling of DT and various drum separators. This was done via three-dimensional mapping and modelling of the magnetic field of a DT and 4 BaFe drum separators, with different magnet configurations resulting in different magnetic field patterns. It was found that the force index is responsible for the separation efficiency, not the magnetic field intensity. Furthermore, the magnet configuration of the drum separator greatly influences the magnetic gradient of the device, which is the magnetic intensity across the distance from the surface of the drum (Murariu & Svoboda, 2003). While both the DT and drum separators have been theoretically modelled separately, the inter-relation and practical relationship between these magnetic separators have not been explored.

2. METHODOLOGY

Two low-grade magnetite ores were subjected to characterization, followed by laboratory magnetic separation testwork to determine how the ore characteristics influence beneficiation, in terms of iron grade and recovery. Each ore was first sub-sampled for characterization, after which it was subjected to Davis tube testwork at various magnetic field intensities. The differences between the grade-recovery profiles of each ore were analysed based on initial ore characterization. Both ores were then subjected to multi-stage WLIMS to determine how the ore characteristics affects recovery. The intention is to use this laboratory data amongst other tests to model pilot scale performance.

2.1. Sample Receipt & Preparation

Two magnetite samples, originating from Mozambique and the Bushveld Complex in South Africa, were received at a maximum size of -1180 µm. Each sample was blended and subsamples were removed for triplicate head assay, duplicate particle size distribution (PSD) and size by assay (SBA), and laboratory magnetic separation testwork, namely DT and WLIMS. The subsamples for laboratory magnetic separation were milled to 85% passing 45 µm.

2.2. Characterization

Three representative 200 g samples of each ore were pulverized for triplicate chemical analysis. Two representative 1 kg subsamples of each ore were subjected to a sieve analysis, from 1180 to 38 µm following the root 2-series, and each size fraction was pulverized for

chemical analysis. Finally, mineralogical analysis, which included Auto Scanning Electron Microscopy (AutoSEM) and Electron Micro Probe Analysis (EMPA) was performed on representative 1kg subsamples.

2.3. Milling for Laboratory Magnetic Separation Testwork

Representative 1 kg subsamples of each sample was subjected to dry balling milling, and at specific time intervals, the percentage passing 45µm was measured and recorded to generate a milling curve. The milling curve was used to determine the milling time to achieve a grind of 85% passing 45 µm. Once the correct milling time was established, 1kg batches were milled, blended and subsampled for magnetic separation testwork.

2.4. Magnetic Separation Testwork

2.4.1. DT testwork

Representative 1 kg subsamples of the milled feed were split into representative 100 g subsamples which were subjected to Davis tube testwork at varying intensities to generate a grade-recovery curve.

2.4.2. WLIMS testwork

Representative 5 kg subsamples of the milled feed were subjected to 4-stage WLIMS testwork, with a circuit comprising of a rougher, cleaner, scavenger and recleaner stages. The drum was operated in a co-current configuration, to increase the residence time of the particles within the tank and maximize Fe grade.

2.5. Model Development

The aim of the model is to use the data generated during DT bench-scale testing to predict WLIMS performance. The basis for the model is explained below.

When exposed to an applied magnetic field, fast flocculation occurs due to a high concentration of magnetic materials in the solids, which leads to the instantaneous capture of magnetic particles, resulting in high capture efficiency. This process is governed by the magnetic susceptibility, rather than size, of the particle. Furthermore, an increase in pick-up gap increases the residence time in the collection zone and reduces the average magnetic

intensity index in the collection zone. However, when low intensity fields are used, flocculation still proceeds quickly, indicating that a lower magnetic intensity does not significantly reduce recovery. In addition, an increased residence time enables the recovery of magnetics that are not immediately captured; however, it unfortunately leads to reduced performance at high feed rates. At low solids concentration, slurry density is low and the flocculation rate is too low to form stable flocculants, thus, particles are captured individually. This causes losses of very fine particles as they are less susceptible to capture due to increased distance. Thus, based on these principles, to ensure optimum collection of magnetics, maintain a small pick-up gap and ensure material is in close proximity to the magnet when the residence time is high (Rayner & Napier-Munn, 2003).

This concept was mathematically modelled by Rayner & Napier-Munn (2003):

$$\frac{N}{N_0} = e^{-kt} \qquad (1)$$

Where:

N is the number of particles remaining un-flocculated,

N_0 is the number of particles at the start of flocculation,

k is a first order rate constant (s^{-1}), and

t is the flocculation time (s).

Since magnetic recovery is a flocculation process, the proportion of unflocculated particles is equivalent to the loss. Thus, the fractional loss (L) is given by:

$$L = e^{-k\frac{V}{Q_f}} \qquad (2)$$

Where:

Q_f is the volumetric feed rate per unit length ($m^3/h/m$), and

V is the volume of the separation zone per unit length (m^3/m), which is given by:

$$V = \theta D x_p \qquad (3)$$

Where:

θ is the angular extent of the separation zone (rad),

D is the drum diameter (m), and

x_p is the pickup gap (m), that is, the distance between the surface of the drum and the bottom of the tank on the product discharge end.

The term θ may be assumed to be a constant for a full length weir overflow magnetic separator.

The rate constant, k, is represented in terms of feed, design and operating variables as a parameterized model derived from dimensional analysis:

$$k = a\frac{Q_f}{D^2}C^b\alpha^c\left(\frac{D^2\omega}{Qf}\right)^d\left(\frac{x_p}{D}\right)^e\left(\frac{\rho_s}{\rho_f}\right)^f Ø^g\left(\frac{\rho_f Q_f}{\mu}\right)^h \quad (4)$$

Where:

C is the non-magnetics contamination (w/w),

α is the magnetic volume susceptibility,

D is the drum diameter (m)

ω is the rotational velocity of the drum (rad/s),

Ø is the volume concentration of solids,

ρ_s is the density of the magnetic solids (kg/m^3),

ρ_f is the density of the feed slurry (kg/m^3),

μ is the slurry viscosity in the pickup zone (Pa.s), and

a–h are parameters to be fitted, contingent upon the aforementioned operating parameters.

The last term in Eq (4) is effectively a Reynolds number (Perry, et al., 1997). As such, the loss function (L) is now given by:

$$L = \exp\left(-\frac{\theta Dxp}{Qf}a\frac{Qf}{D^2}C^b\alpha^c\left(\frac{D^2\omega}{Qf}\right)^d\left(\frac{xp}{D}\right)^e\left(\frac{\rho_s}{\rho_f}\right)^f Ø^g\left(\frac{\rho_f Qf}{\mu}\right)^h\right) \quad (5)$$

The non-parameterized terms $\frac{\theta Dxp}{Qf}$ $a\frac{Qf}{D^2}$ can be reduced to $a\frac{\theta xp}{D}$. The terms a and θ cannot be independently fitted, thus, they can be combined into one constant, a.

There is also $a\frac{xp}{D}$ term with an adjustable parameter, a, the $\frac{xp}{D}$ component may be included in this revised fitted term, a.

As a result, the loss function (L) is reduced to:

$$L = \exp\left(-aC^b\alpha^c\left(\frac{D^2\omega}{Qf}\right)^d\left(\frac{xp}{D}\right)^e\left(\frac{\rho_s}{\rho_f}\right)^f \emptyset^g\left(\frac{\rho_f Qf}{\mu}\right)^h\right) \quad (6)$$

Finally, recovery, R, is given by:

$$R = 1 - L \qquad (7)$$

Where:

R is the recovery of Fe to the magnetic concentrate.

All other terms are operating parameters that will be measured during testwork, and the parameters a-h will be fitted to the equation for various data sets to further simplify the model.

Once the R model is established, each term will be incrementally step changed positively and negatively, and the resulting R will be recorded. The weighted analysis of each of the terms and the proportion of significance they ascribed to the overall model will be used to develop a predictive magnetic mass yield model given by:

$$MY = (MY_{DTR} lnFe_{DTR})^{a'} (D\omega)^{b'} (\frac{\rho_f \emptyset}{\mu})^{c'} \alpha^{d'} R^{e'} \quad (8)$$

Where:

MY is the magnetic mass yield expected from a single stage WLIMS drum,

MY_{DTR} is the resultant magnetic mass yield from a DTR test at 1000 Gauss on the same material,

Fe_{DTR} is the Fe grade of the magnetic DTR product,

R is the WLIMS Fe recovery predicted from equation 7, and

a'-e', were fitted to the equation in a similar manner as those for equation 6.

3. RESULTS AND DISCUSSION

3.1. Characterization

The head assay for Magnetite 1 and Magnetite 2 are presented in Table 1.

Table 1: Head assay of Magnetite 1

	Al2O3 %	CaO %	Cr2O3 %	Fe(Total) %	K2O %	MgO %	MnO %	P2O5 %	SiO2 %	TiO2 %	V2O5 %
Magnetite 1	0.96	2.97	<0.05	53.1	0.35	7.59	0.28	1.36	5.81	3.76	0.17
Magnetite 2	0.70	6.22	0.05	55.8	0.13	4.93	0.25	1.44	3.00	2.35	0.14

The results indicate that the Fe grade of Magnetite 1 (53.1%) is slightly lower than that of Magnetite 2 (55.8%). In addition, Magnetite 1 has a higher TiO_2 content (3.76%) than Magnetite 2 (2.35%). The major gangue in both samples include CaO, MgO and SiO_2, however, Magnetite 1 has more MgO (7.59%), followed by SiO_2 (5.81%) and CaO (2.97%) whereas Magnetite 2 has more CaO, followed by MgO (4.93%) and SiO_2 (3.00%).

The discrete particle size distribution for both magnetite samples, shown in Figure 3, indicates that Magnetite 1 has a higher degree of coarse particles, with majority of particles reporting to the -425+150 µm size fractions, whereas Magnetite 2 has majority of particles reporting to the -300+106 µm fraction, indicating more finer particles. However, the slimes fraction (-38 µm) is similar for both size fractions, with slightly more slimes in Magnetite 2 (4.21% vs. 3.80%). The cumulative particle size distribution is presented in Figure 4, and it shows that Magnetite 2 is finer than Magnetite 1 as the % passing any given size is higher for Magnetite

2. Furthermore, Magnetite 2 has a steep gradient in the lower size ranges (<300 µm), indicating a narrow size distribution of these particles. Whereas the gradient for Magnetite 1 is more gradual, which suggests a wide size distribution, and a generally coarser feed. This is confirmed by higher D_{50} and D_{80} values for Magnetite 1 (D_{50}= 135 µm; D_{80}= 278 µm) than Magnetite 2 (D_{50}= 130 µm; D_{80}= 253 µm).

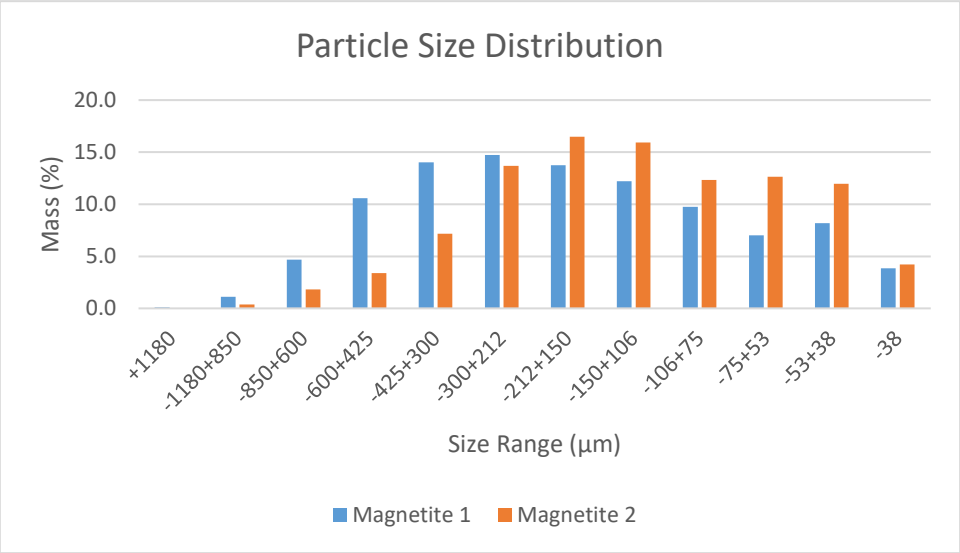

Figure 3: Discrete particle size distribution

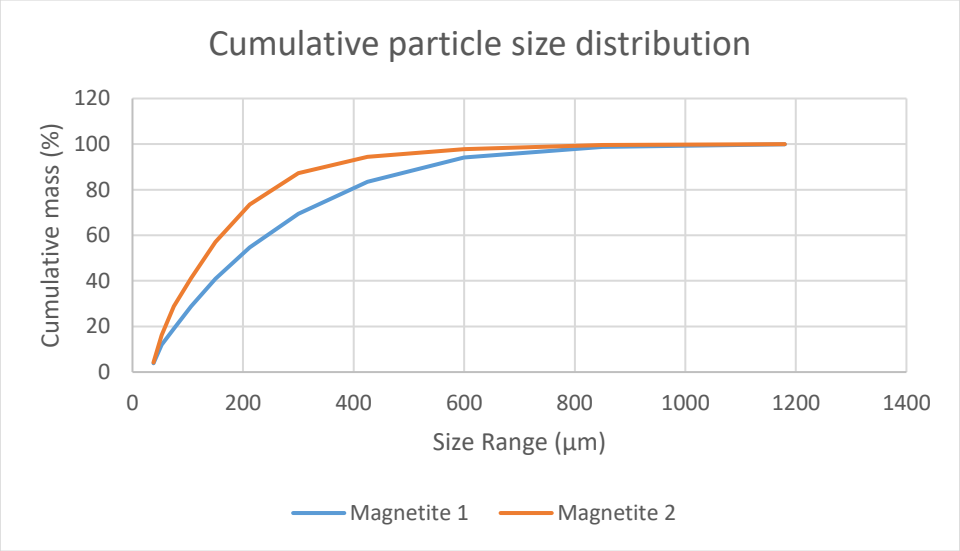

Figure 4: Cumulative particle size distribution

The Fe grade across size and the Fe deportment across size for both samples is presented in Figure 5 and Figure 6, respectively. Figure 5 shows that the Fe grades for Magnetite 1 remain relatively constant, ranging from 44.6-55.2%, with the maximum %Fe in the -425+300 µm size range. Furthermore, Figure 6 indicates that Fe deportment closely follows mass pull due to

the relatively constant grade. Whereas the Fe grades of Magnetite 2 increase with decreasing size, ranging from 12.1-62.0%, with the maximum %Fe in the -53+38 µm and -38 µm size ranges. The Fe deportment follows mass pull, however, due to increasing deportment with decreasing size, coarser fractions (+300 µm) contain less than 10% Fe combined. Both samples have ~4.4%Fe reporting to the slimes (-38 µm) fraction.

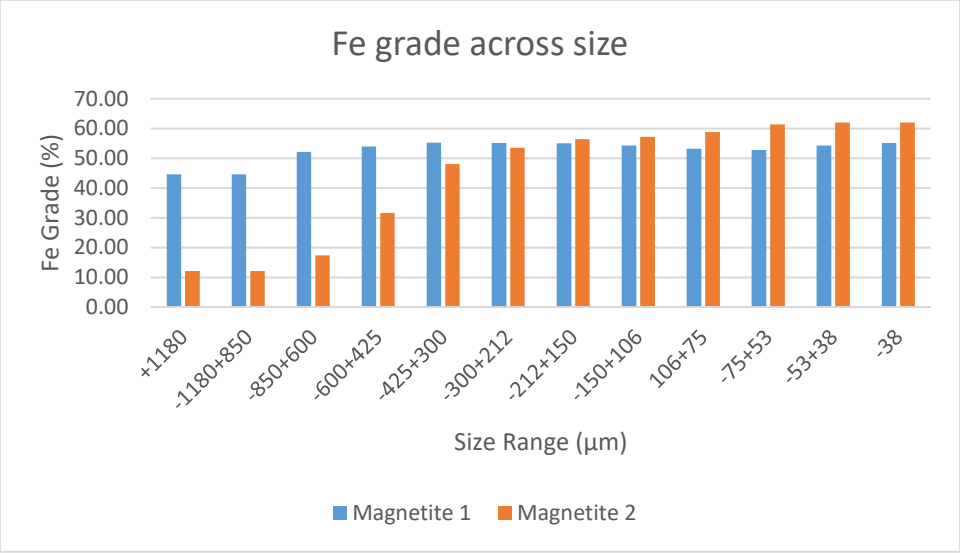

Figure 5: Fe grade across size

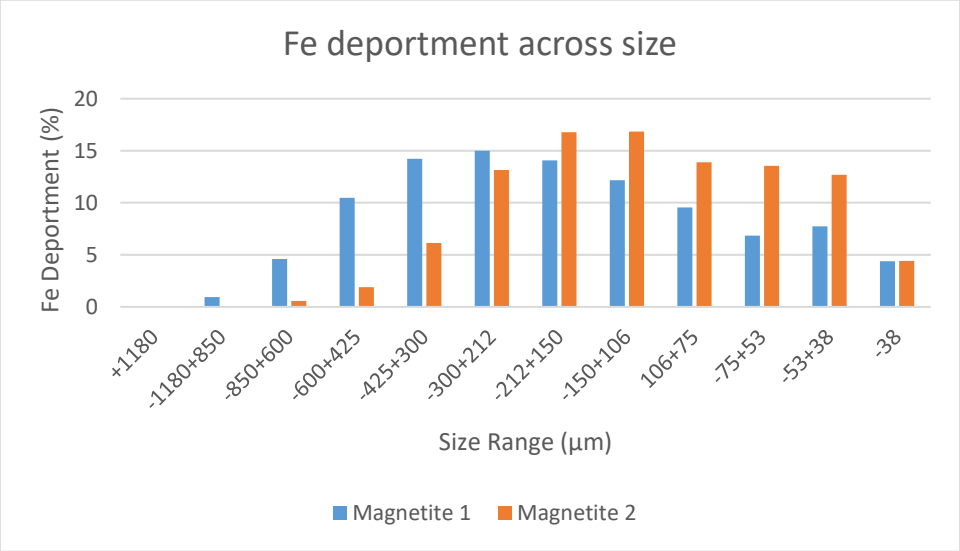

Figure 6: Fe deportment across size

Mineralogical analysis revealed that there are five magnetite bearing phases present in both magnetite ores. The mass distribution and Fe deportment of these phases are presented in Table 2.

Table 2: Mass distribution and Fe deportment of magnetite-bearing phases

Phases	Magnetite 1		Magnetite 2	
	Mass %	Fe deportment %	Mass %	Fe deportment %
Magnetite - Clean	9.24	12.5	14.4	18.9
Magnetite - Clean with High Ti	7.78	8.45	2.25	2.38
Magnetite - Clean with Low Ti	31.1	39.5	25.8	31.9
Magnetite - Cross-hatched exsolution	24.5	28.4	25.8	29.1
Magnetite - Spotted exsolution	5.82	7.32	12.9	15.8
TOTAL	**78.46**	**96.14**	**81.18**	**98.09**

The mass distribution of both ores indicate that magnetite clean with low Ti is the dominant mineral phase, flowed by magnetite cross-hatched exsolution and magnetite clean. Fe deportment follows a similar trend. The identified phases are shown in Figure 7 and Figure 8 for Magnetite 1 and Magnetite 2, respectively. Furthermore, for Magnetite 1, magnetite particles were moderate to well liberated at more than 77mass% >80% liberated and grain size distribution indicated that 30-65mass% of these phases are ≤150 µm. For Magnetite 2, magnetite particles are well liberated with more than 80mass% >80% liberated and, in terms of grain size distribution, ~65-72mass% of these phases are ≤150 µm. For both ores, when not

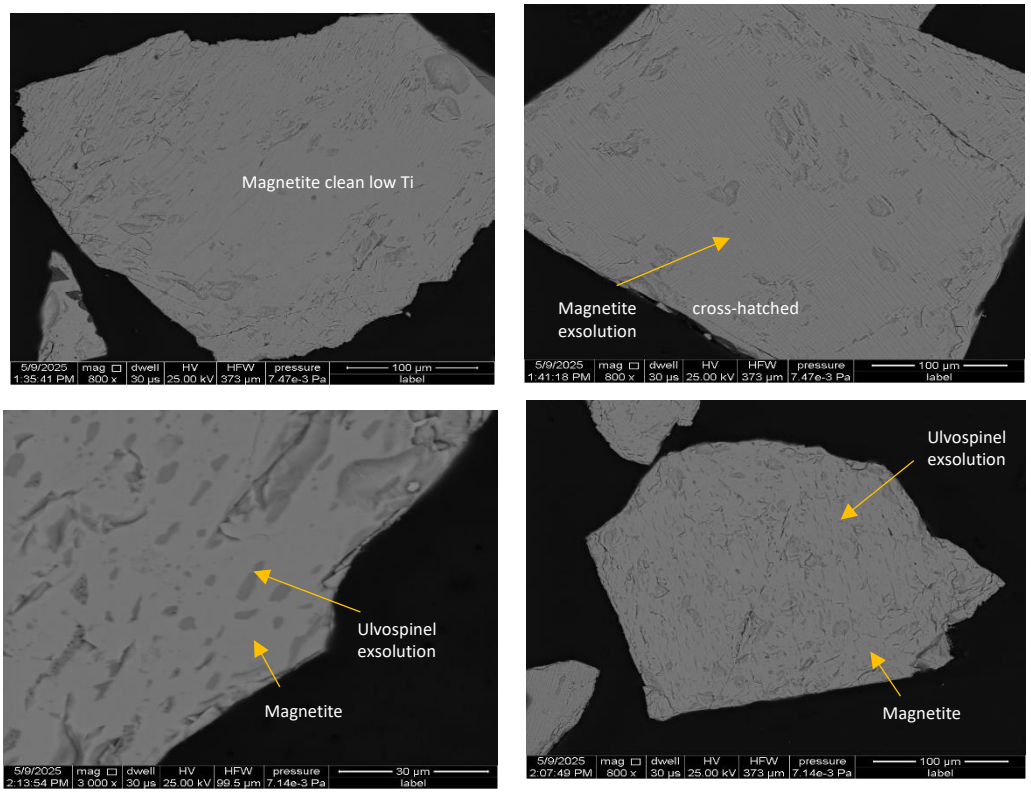

Figure 7: AutoSEM images of Magnetite 1

well liberated, magnetite is associated with serpentine, olivine, talc, carbonates, rutile, ilmenite, biotite and apatite.

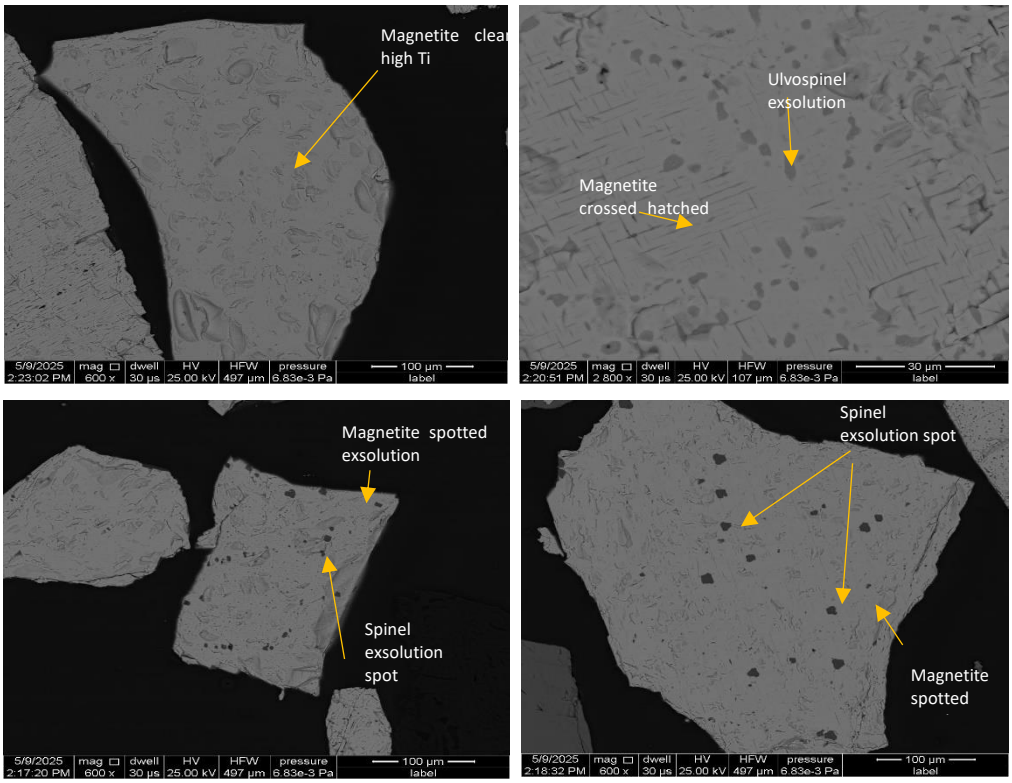

Figure 8: AutoSEM images of Magnetite 2

3.2. Milling for Laboratory Magnetic Separation Testwork

The milling curves for both samples are presented in Figure 9, and they indicate that Magnetite 1 requires a milling time of 40 minutes 55 seconds and Magnetite 2 requires a lower milling time of 36 minutes 32 seconds to achieve 85% passing 45 µm due to it being finer.

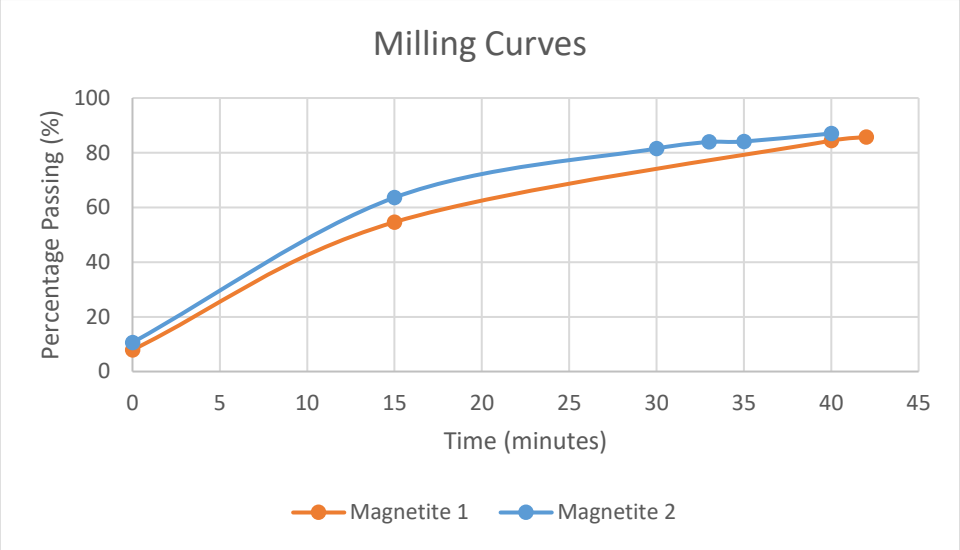

Figure 9: Milling curves for Magnetite 1 and Magnetite 2

3.3. Magnetic Separation Testwork

3.3.1. DT vs. WLIMS testwork

Extensive DTR testwork was performed to benchmark possible achievable grades and recoveries on two magnetite ores. The objective of this testwork is to compare how both magnetite ores responds to DTR and WLIMS, in terms of mass yield, grade and recovery.

The DTR results for Magnetite 1 is presented in Table 3.

Table 3: DTR results for Magnetite 1

Magnetic Intensity (Gauss)	Mass Yield (%)	Fe Grade (%)	Fe Recovery (%)	CaO Grade (%)	MgO Grade (%)	SiO_2 Grade (%)
1046	72.2	65.3	86.4	0.49	3.21	1.91
2060	75.5	64.1	89.1	0.68	3.26	2.07
2960	78.1	63.3	90.7	0.77	3.48	2.47
3990	82.7	62.6	92.9	1.01	3.59	2.79

At 1046 Gauss, Magnetite 1 achieved a Fe grade of 65.3%, at a mass yield of 72.2% and recovery of 86.4%. The associated CaO, MgO and SiO_2 grades are 0.49%, 3.21% and 1.91%, respectively, and they remain relatively constant across intensities, with the exception of CaO. The mass yields for the varying intensities range from ~72% to ~83%. At the maximum intensity, i.e. 3990 Gauss, the lowest Fe grade (62.6%), and highest mass yield (82.71%) and recovery (95.8%) is achieved. Table 4 presents comparative DTR and WLIMS results for Magnetite 1.

Table 4: Comparative DTR and WLIMS results for Magnetite 1

Multi-stage WLIMS vs DTR	Magnetics					
	Overall Mass yield (%)	Fe Grade (%)	Overall Fe Recovery (%)	CaO Grade (%)	MgO Grade (%)	SiO2 Grade (%)
Rougher Stage WLIMS	83.0	60.0	92.6	1.25	4.71	2.90
Cleaner Stage WLIMS	76.4	62.2	87.8	0.72	4.02	2.09
Recleaner Stage WLIMS / Overall WLIMS performance	75.1	62.6	86.7	0.56	3.79	2.01
DTR @ 1000 Gauss	72.2	64.3	86.4	0.49	3.79	1.91
Standard error (%)	3.82	2.72	0.31	12.5	0.00	4.98

The rougher WLIMS stage at 1000 Gauss achieved a mass yield of 83.0%, which was significantly greater than DTR at 1046 Gauss (72.19%), confirming that separation efficiency cannot be determined by only magnetic strength (Murariu & Svoboda, 2003). However, when compared to a 3-stage WLIMS, including a rougher, cleaner and recleaner, similar results are achieved. The overall WLIMS circuit achieve a mass yield of 75.1, which is slightly higher than that of the 1046 Gauss DTR results (72.2%). The circuit produced an overall grade and recovery of 62.6% and 86.7%, respectively, in comparison to a grade and recovery of 64.3% and 86.4%, respectively, produced by DTR testwork. Furthermore, the mass yield and recovery achieved for the rougher WLIMS stage corresponds to results achieved for DTR at 3990 Gauss, with the DTR grade slightly higher (62.6% vs. 60.0%) reasonably so since DT are used as a benchmark for optimum grade and recovery achievable.

The DTR result for Magnetite 2 is presented in Table 5.

Table 5: DTR results for Magnetite 2

Magnetic Intensity (Gauss)	Mass Yield (%)	Fe Grade (%)	Fe Recovery (%)	CaO Grade (%)	MgO Grade (%)	SiO_2 Grade (%)
1046	68.9	66.5	86.4	2.47	4.20	1.42
2060	78.1	66.1	91.4	2.63	4.32	1.48
2960	83.9	65.5	95.2	2.97	4.43	1.64
3990	86.7	62.8	96.7	3.05	4.57	1.79

Magnetite 2 achieved a slightly higher grade than Magnetite 1, which can be attributed to its slightly higher head grade (55.8% v 53.1% Fe). At 1046 Gauss, the grade of Magnetite 2 is 66.5%, with a corresponding mass yield of 68.9% and a recover of 86.4%. The CaO, MgO and SiO_2 grades at 1046 Gauss are 2.47%, 4.20% and 1.42%, respectively, and they also remain

relatively constant across intensities. The mass yields for Magnetite 2 range from ~69% to ~87%. At the maximum intensity, i.e. 3990 Gauss, the Fe grade is significantly lower at 62.8%, however, it corresponds to the highest mass yield (86.7%) and recovery (96.7%). The reduced grade in both ores at 3990 Gauss may be a result of attracting magnetite with intergrown gangue as depicted by mineralogy.

The comparative DTR and WLIMS results for Magnetite 2 is presented in Table 4.

Table 6: Comparative DTR and WLIMS results for Magnetite 2

Multi-stage WLIMS vs DTR	Magnetics					
	Overall Mass yield (%)	Fe Grade (%)	Overall Fe Recovery (%)	CaO Grade (%)	MgO Grade (%)	SiO2 Grade (%)
Rougher Stage WLIMS	85.6	63.3	96.9	2.32	3.41	1.60
Cleaner Stage WLIMS	75.5	66.2	89.0	1.22	3.29	0.94
Recleaner Stage WLIMS / Overall WLIMS performance	72.8	66.4	86.5	0.84	3.02	0.67
DTR @ 1000 Gauss	68.9	66.5	86.4	1.04	2.99	0.75
Standard error (%)	4.15	0.15	0.12	23.96	0.99	11.9

The mass yield for WLIMS rougher stage is 85.6%, which is also greater than DTR at the same intensity (68.9%). However, as with Magnetite 1, the 3-stage WLIMS achieves results in a reduced mass yield of 72.8%. More material reports to the magnetic fraction during WLIMS, which may be due to the Davis tube being designed for optimum separation leading to lower mass yields, whereas drum separators are designed to maximize recovery. The 3-stage WLIMS also achieved a Fe grade of 66.4% at an overall recovery of 86.5%, which differs from DTR results by 0.1%. Similarly, the mass yield and recovery achieved for the rougher WLIMS stage also corresponds to results achieved for DTR at 3990 Gauss, with the WLIMS grade slightly higher (63.3% vs. 62.8%).

These correlations confirm that separation efficiency depends on the force index (Murariu & Svoboda, 2003), thus, different separators will require different magnetic intensities to achieve the same results. This data indicates that results achieved for DTR at 1046 Gauss correlates to a 3-stage WLIMS circuit, and the results for rougher WLIMS at 1000 Gauss corresponds to DTR at ~4000 Gauss.

3.4. Model development

The operating conditions, the results obtained from this testwork and the correlations determined during this testwork will be used as different parameters in the loss equation (Equation 6) to develop a recovery model (Equation 7), which will then be used to develop the mass yield model (Equation 8). The final outcome will be a predictive model to determine WLIMS pilot performance from only DTR data.

4. CONCLUSIONS & RECOMMENDATIONS

Two low grade (<60% Fe) magnetite ores were used, with a Fe content of 53.1% and 55.8% for Magnetite 1 and Magnetite 2, respectively. The PSD and SBA analysis indicate that Magnetite 1 is coarser than Magnetite 2. Both samples were then milled to 85% passing 45 µm in preparation for magnetic separation testwork. DTR testwork was performed at various intensities, followed by 3-stage WLIMS testwork and a comparative analysis to assess the response of both magnetite ores to DTR and WLIMS testwork, in terms of mass yield, grade and recovery. The results show that similar trends are observed for both magnetite ores. DTR at 1046 Gauss does not produce the same results as rougher WLIMS at 1000 Gauss, which indicates that magnetic intensity is not responsible for separation efficiency. However, DTR results at ~1000 Gauss correlates to a 3-stage WLIMS circuit, and the results for rougher WLIMS at 1000 Gauss corresponds to DTR at ~4000 Gauss, thus, force index has the biggest influence on separation efficiency as different units achieve different results at the same intensity.

ACKNOWLEDGEMENTS

The authors would like to acknowledge Mintek for funding the research project and providing the facilities and resources required to complete this study. The authors would also like to thank Mintek's mineralogical and analytical division for their contribution to this research.

REFERENCES

Eriez. (2024). *Eriez Magnetic Drum Separators*. Retrieved 05 20, 2024, from https://www.eriez.com/NA/EN/Products/Magnetic-Separation/Permanent-Magnets/Drum-Separators.htm

Jain, P., Bhattacharya, S., & Kumar, S. (2016). Recovery of combustibles from electrostatic precipitator discharge. *Waste Management & Research, 34*(6), 542-552.

Murariu, V., & Svoboda, J. (2003). The applicability of Davis Tube tests to ore separation by drum magnetic separators. *Physical Separation in Science and Engineering*, 1-11.

Perry, R., Green, D., & Maloney, J. (1997). *Perry's Chemical Engineers' Handbook* (7th ed.). New York: McGraw Hill.

Rayner, J., & Napier-Munn, T. (2000). Mathematical Models of the Wet Drum Magnetic Separator. Durban: Samancor.

Schulz, N. (1963). Determination of the Magnetic Separation Characteristic with the Davis Magnetic Tube . Salt Lake City : Society of Mining Engineers of AIME.

Steinhart, H., & Boehm, A. (2000). Prediction of the performance of wet low intensity magnetic separators in the processing of partly altered magnetite ores. Rome: Elsevier.